LETTER

doi:10.1038/nature13823

Rapid fucosylation of intestinal epithelium sustains host–commensal symbiosis in sickness

Joseph M. Pickard[1], Corinne F. Maurice[2], Melissa A. Kinnebrew[3], Michael C. Abt[3], Dominik Schenten[4], Tatyana V. Golovkina[5], Said R. Bogatyrev[6], Rustem F. Ismagilov[6], Eric G. Pamer[3], Peter J. Turnbaugh[2] & Alexander V. Chervonsky[1]

Systemic infection induces conserved physiological responses that include both resistance and 'tolerance of infection' mechanisms[1]. Temporary anorexia associated with an infection is often beneficial[2,3], reallocating energy from food foraging towards resistance to infection[4] or depriving pathogens of nutrients[5]. However, it imposes a stress on intestinal commensals, as they also experience reduced substrate availability; this affects host fitness owing to the loss of caloric intake and colonization resistance (protection from additional infections)[6]. We hypothesized that the host might utilize internal resources to support the gut microbiota during the acute phase of the disease. Here we show that systemic exposure to Toll-like receptor (TLR) ligands causes rapid α(1,2)-fucosylation of small intestine epithelial cells (IECs) in mice, which requires the sensing of TLR agonists, as well as the production of interleukin (IL)-23 by dendritic cells, activation of innate lymphoid cells and expression of fucosyltransferase 2 (Fut2) by IL-22-stimulated IECs. Fucosylated proteins are shed into the lumen and fucose is liberated and metabolized by the gut microbiota, as shown by reporter bacteria and community-wide analysis of microbial gene expression. Fucose affects the expression of microbial metabolic pathways and reduces the expression of bacterial virulence genes. It also improves host tolerance of the mild pathogen *Citrobacter rodentium*. Thus, rapid IEC fucosylation appears to be a protective mechanism that utilizes the host's resources to maintain host–microbial interactions during pathogen-induced stress.

To maintain healthy gut microbiota during a systemic response induced by microbial products the host may use its internal resources. L-Fucosylation could present an example of such a resource: L-fucose attached to glycoproteins and glycolipids is accessible for microbial, but not for host energy harvest[7,8]. Constitutive α(1,2)fucosylation affects the microbial community in a diet-dependent manner[9], serves as a substrate for pathogens during antibiotic exposure[10] and for microbes colonizing the ileum of newborns or of adult germ-free (GF) mice[11–13]. Under normal conditions, however, the small intestine of specific pathogen-free (SPF) BALB/c mice is largely free of surface fucose. By contrast, a systemic injection of agonists of TLRs, such as lipopolysaccharide (LPS; TLR4 ligand) (Fig. 1), CpG DNA (TLR9 ligand), or Pam_3CSK_4 (TLR2 agonist), led to ubiquitous α(1,2)fucosylation of the small intestine in mice of different genetic backgrounds, which started within a few hours after LPS exposure and lasted for several days (Extended Data Fig. 1a–c). It did not result in differentiation of IECs into functional M cells[14], which are permanently fucosylated and are involved in microbial sensing and translocation (Extended Data Fig. 1d). Induced fucosylation was independent of the gut microbiota (observed in GF mice), and was not induced by oral LPS (Extended Data Fig. 1e).

Global deletion of the TLR signalling adaptor molecule MyD88 prevented IEC fucosylation, and its conditional deletion from dendritic cells, but not from IECs, abrogated the process (Fig. 1). The inducible fucosylation pathway was similar to induction of antimicrobial peptides by a systemic microbial signal[15]: it required MyD88-expressing dendritic cells, production of IL-23, the transcriptional regulator RORγt and IL-22 (Fig. 1 and Extended Data Fig. 2a), and was induced by a direct injection of IL-22 into *Myd88*$^{-/-}$ mice (Fig. 1). IEC fucosylation in mice lacking T cells (Fig. 1) suggested that innate lymphoid cells (ILCs) were a sufficient source of IL-22. *Salmonella enterica* ssp. Typhimurium, known to spread systemically, induced small intestine IEC fucosylation (Extended Data Fig. 2b). The α(1,2)fucosyltransferase responsible for fucosylation of IECs in the small intestine was identified as Fut2 (Fig. 2a), which is inducible by stress conditions[16,17] and constitutively expressed in the stomach and large intestine[18]. Genetic ablation of the *Fut2* gene blocked IEC fucosylation in response to LPS (Fig. 2b, c). The overall chain of events is shown in Extended Data Fig. 3.

LPS injection caused marked sickness in BALB/c Fut2-deficient (*Fut2*$^{-/-}$) and Fut2-sufficient (*Fut2*$^{+/+}$ or *Fut2*$^{+/-}$) littermates hours after injection: mice displayed measurable anorexia, adipsia, reduced activity, diarrhoea and weight loss. Food consumption, weight loss, and production of inflammatory cytokines and antimicrobial peptides (Fig. 2d, e and Extended Data Fig. 4a, b) were similar in both groups. Although

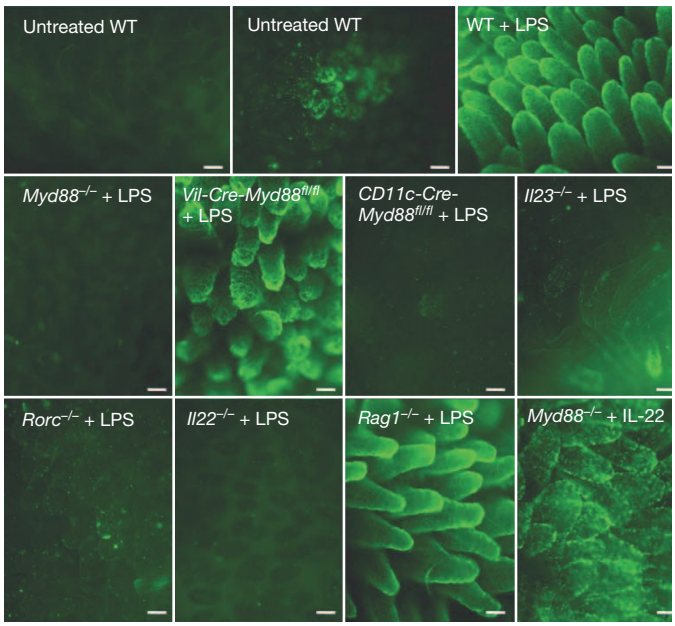

Figure 1 | MyD88-dependent fucosylation of small intestine IECs by systemic stimulation of TLRs. UEA-1, which binds α(1,2)-fucosylated substrates, staining in the proximal one-third of the small intestine of mice untreated or 24 h after intraperitoneal (i.p.) LPS injection, or 6 h after injection of IL-22 (*Myd88*$^{-/-}$ mouse). Scale bars = 100 μm. Staining of tissue from mutant mice was always accompanied by staining of wild-type (WT) controls, and is representative of at least two independent experiments for each genotype.

[1]Department of Pathology and Committee on Immunology, The University of Chicago, Chicago, Illinois 60637, USA. [2]FAS Center for Systems Biology, Harvard University, Cambridge, Massachusetts 02138, USA. [3]Memorial Sloan-Kettering Cancer Center, New York, New York 10065, USA. [4]The University of Arizona, Tucson, Arizona 85721, USA. [5]Department of Microbiology, The University of Chicago, Chicago, Illinois 60637, USA. [6]California Institute of Technology, Pasadena, California 91125, USA.

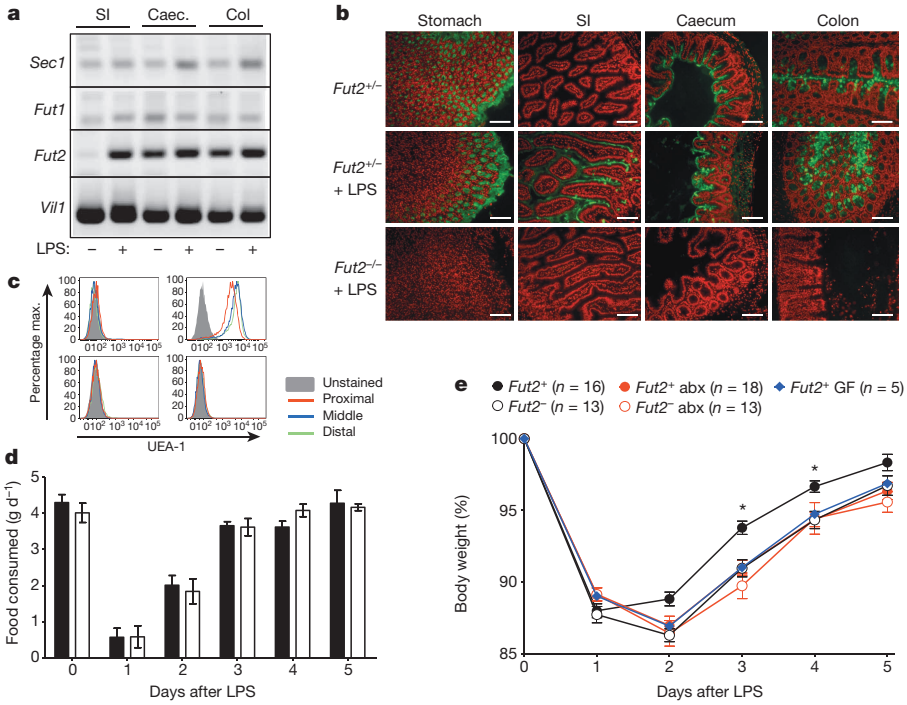

Figure 2 | Consequences of the loss of Fut-2-dependent fucosylation. **a**, Expression of mouse α(1,2)fucosyltransferase genes (*Fut2*, *Fut1* and *Sec1*) and control (villin-encoding gene, *Vil1*) in the gut 24 h after LPS injection (semiquantitative polymerase chain reaction with reverse transcription (RT–PCR)). Caec, caecum; Col., colon; SI, small intestine. **b**, Intestinal fucosylation (green) of Fut2-sufficient and Fut2-deficient mice. Red, propidium iodide. Scale bars = 100 μm. **c**, Fluorescence-activated cell sorting (FACS) histograms of small intestine IECs from PBS- (left) or LPS- (right) injected, $Fut2^{+}$ (top) or $Fut2^{-}$ (bottom) mice. **d**, Food consumption in LPS-treated $Fut2^{+}$ ($n = 5$, black bars) and $Fut2^{-}$ mice ($n = 3$, open bars) (mean ± standard error of the mean (s.e.m.)). **e**, Dependence of weight recovery after LPS challenge on the presence of microbiota and expression of Fut2 (mean ± s.e.m. of percentage of starting body weight, data combined from four experiments). *$P < 0.05$, one-way ANOVA. abx, antibiotics (ampicillin and vancomycin). All data are representative of at least two independent experiements.

$Fut2^{-/-}$ mice have been shown to be healthy under normal SPF conditions[19], they were significantly slower than controls in recovering their body weight (Fig. 2e) after LPS injection. Importantly, food deprivation without LPS challenge did not cause small intestine fucosylation and the weight recovery was identical in Fut2-sufficient and Fut2-deficient animals (Extended Data Figs 1a and 4c). Thus, fucosylation of the small intestine was a response to activation by microbial stimuli and not to anorexia per se.

To understand the reason for the slow weight recovery in $Fut2^{-/-}$ mice, we tested whether fucosylation affected the function of host IEC proteins, which were identified by direct sequencing as secreted mucins and digestive enzymes (Fig. 3a). Fucosylation did not change the activity of several enzymes (Fig. 3b). Thus, changes in enzymatic activity are unlikely to explain the slow weight recovery in $Fut2^{-/-}$ mice, although the role of less abundant fucosylated proteins cannot be excluded.

The beneficial effect of fucosylation was dependent on the microbiota: the weight recovery after LPS challenge was delayed in GF mice and in wild-type SPF mice treated with antibiotics (Fig. 2e). Antibiotics did not have a direct effect on the host's responses to LPS (Extended Data Fig. 4a, b, d–g) and did not further impair the recovery of $Fut2^{-/-}$ mice (Fig. 2e). Thus, Fut2 and an intact gut microbiota were both necessary for efficient recovery of body weight after LPS challenge.

To serve as a substrate to the bacteria residing in the large intestine[20], fucosylated proteins (Extended Data Fig. 5a–d) must be released into the small intestine lumen. After LPS challenge, Fut2-dependent fucosylation of luminal proteins was detectable at much higher levels in GF mice and in SPF mice treated with antibiotics or with a fucosidase inhibitor, than in SPF controls (Fig. 3c and Extended Data Fig. 5e). Thus, fucose is available, released and used by microbes in the large intestine.

Next, to directly show fucose sensing by intestinal commensal bacteria, we used a reporter system in which *Escherichia coli* expressed green fluorescent protein (GFP) driven by the promoter of the *E. coli* fucose metabolism operon[21,22] (Fig. 3d, e and Extended Data Fig. 6a). Because *E. coli* lacks α(1,2)fucosidase that cleaves fucose off substrates, in GF mice monocolonized with the reporter *E. coli* it did not upregulate GFP, even after LPS injection (Fig. 3d). Thus, free fucose was not readily available for reporter bacteria in the gut and required bacterial fucosidase activity, which was sensitive to antibiotics (Extended Data Fig. 6b). A commensal bacterium with α(1,2)fucosidase activity, *Bacteroides acidifaciens*, was isolated from our mouse colony (Extended Data Fig. 6c–e). In LPS-injected GF mice co-colonized with the reporter *E. coli* and *B. acidifaciens*, the reporter strain expressed significantly more GFP (Fig. 3d), as well as genes for fucose import (*fucP*) and metabolism (*fucA*) (Fig. 3f). In LPS-treated SPF mice, Fut2 was required for GFP reporter expression (Fig. 3e and Extended Data Fig. 6f). These findings made it clear that fucose can serve as a substrate for the microbiota under conditions of stress applied to the host, and underscored the interdependence between members of the gut microbial community[23].

To confirm these findings in mice with complex gut microbiota, we profiled microbial community structure, gene abundance and transcriptional activity before and after LPS treatment of $Fut2^{+/-}$ and $Fut2^{-/-}$ mice (Supplementary Table 1). Analyses of community structure based on 16S and shotgun DNA sequencing revealed that the gut microbiota was largely robust to host genotype and LPS exposure (Fig. 3g and Extended Data Fig. 7a, b). We did not detect: (1) significant clustering of microbial communities based on genotype or LPS treatment ($P > 0.05$ for both comparisons; permutational multivariate analysis of variance (PERMANOVA) of unweighted UniFrac distances); (2) species-level operational taxonomic units (OTUs) significantly associated with host genotype before or after LPS treatment (all were $q > 0.05$; analysis of variance (ANOVA)); or (3) significant differences in overall microbial diversity (Extended Data Fig. 7c). However, we were able to detect a significantly increased abundance of *B. acidifaciens* after LPS treatment in Fut2-sufficient mice ($P < 0.05$, linear discriminant analysis (LDA) score > 4; linear discriminant analysis effect size (LefSe) analysis of 16S profiles), consistent with its ability to utilize fucosylated glycans.

At the same time, LPS markedly altered community-wide gene expression in both $Fut2^{+/-}$ and $Fut2^{-/-}$ mice (Fig. 3h), with multiple orthologous groups differentially expressed upon LPS treatment: 61 in $Fut2^{+/-}$ mice and 56 in $Fut2^{-/-}$ animals. These changes were not due to altered community structure: only one differentially expressed orthologous group (K05351, xylulose reductase) also exhibited significant changes in gene abundance (Supplementary Table 2). As expected, we detected a significant upregulation of fucose permease (*fucP*; K02429) in Fut2-sufficient mice after exposure to LPS (Fig. 3i), and increased expression of metabolic modules for anaerobic respiration, protein and ATP synthesis, isoprenoid biosynthesis and amino sugar import, in addition to pathways

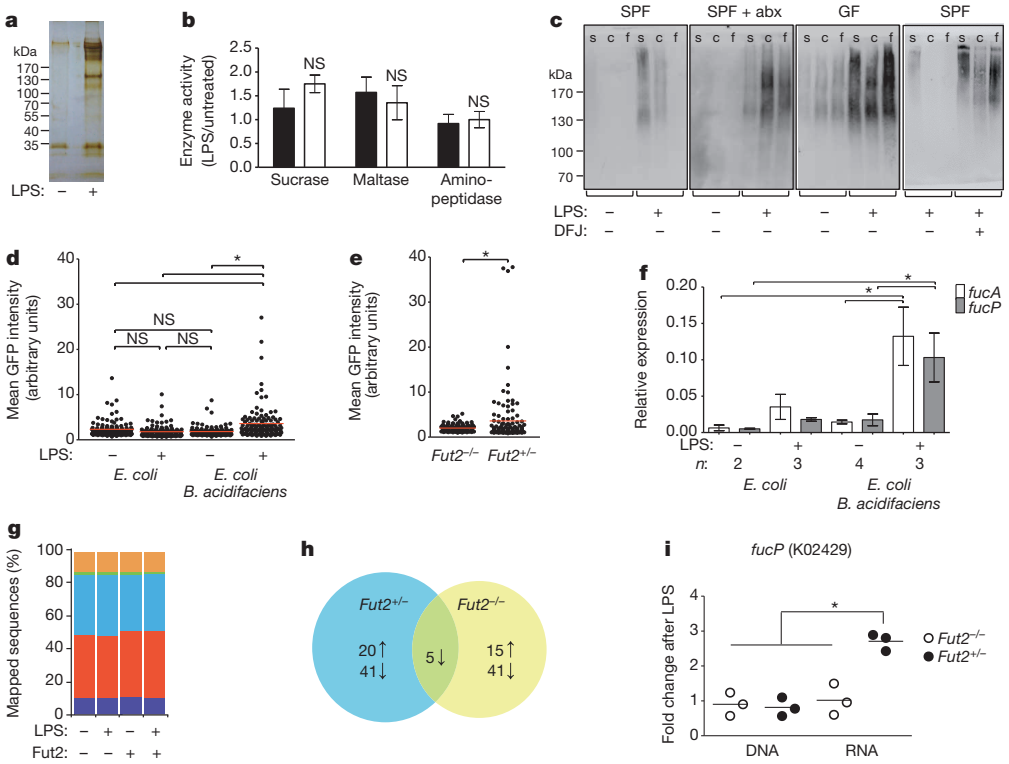

Figure 3 | Commensals utilize fucose detached from proteins fucosylated by Fut2 upon systemic challenge with LPS. **a**, Silver-stained SDS–polyacrylamide gel electrophoresis (SDS–PAGE) of UEA-1-precipitated small intestine IEC protein from control or LPS-treated mouse. **b**, Ratios of digestive enzyme activities in small intestine IECs of LPS-treated to untreated Fut2-sufficient (black bars) or Fut2-deficient (open bars) mice 2 days after LPS injection. Mean ± s.e.m. of four combined experiments; four mice per group. NS, not significant ($P > 0.05$, two-tailed Student's *t*-test). **c**, SDS–PAGE of intestinal contents blotted on nitrocellulose and stained with UEA-1–peroxidase complexes. abx, antibiotic-treated mice; c, caecum; DFJ, deoxyfuconojirimycin; f, faeces; s, small intestine. Data are representative of at least two experiments. **d**, **e**, Fucose-sensitive GFP reporter expression in gnotobiotic mice colonized with the indicated strains (**d**) or SPF mice (**e**). Dots are values for individual bacteria, lines are means; $n = 120$. $^*P < 0.05$, one-way ANOVA with Bonferroni post-test (**d**), two-tailed Student's *t*-test (**e**). Data are representative of three independent experiments. **f**, *fucA* and *fucP* gene expression relative to housekeeping gene *rpoA* (quantitative RT–PCR) in *E. coli* tested as in **d**. $^*P < 0.05$ by ANOVA with Bonferroni's post-test. Data are combined from three experiments. **g**, Stable relative abundance of bacterial phyla across treatment groups and genotypes, as indicated by shotgun sequencing of community DNA. Phyla with a mean reads per kilobase per million mapped reads (RPKM) >40,000 are shown, including Actinobacteria (purple), Bacteroidetes (red), Firmicutes (blue), Fusobacteria (green), Proteobacteria (orange) and Tenericutes (yellow). 16S rRNA gene sequencing confirms these observations. Extended Data Fig. 7 shows 16S rRNA gene sequencing results. **h**, Differentially expressed KEGG orthologous groups following LPS treatment (paired glm edgeR analysis; $q < 0.05$, >2-fold change; see Supplementary Table 2 for complete list). **i**, Increased gut microbial expression of *fucP* (K02429) in Fut2-sufficient mice (mean ± s.e.m.; $^*P < 0.01$, Mann–Whitney test).

for aminoglycan degradation (Extended Data Fig. 7d). Thus, intact host fucosylation appears to affect gut microbial metabolism.

Importantly, LPS challenge led to the significantly increased expression of microbial virulence genes in Fut2-negative but not Fut2-sufficient mice, including *rtxA* (K10953) and haemolysin III (K11068) (Supplementary Table 2). Kyoto Encyclopedia of Genes and Genomes (KEGG) pathways potentially involved in microbial pathogenesis (defined as flagellar synthesis, chemotaxis, plant/pathogen interaction and *Vibrio cholera* infection) were overrepresented in Fut2-deficient mice (Extended Data Fig. 7d). We hypothesized that fucosylation induced by systemic microbial challenge might limit the effects of additional exogenous or endogenous pathogens. We tested this by infecting Fut2-sufficient and Fut2-deficient mice with a non-lethal intestinal pathogen, *C. rodentium*. Four days after infection, mice were treated with LPS. Infected Fut2-negative mice lost significantly more weight than Fut2-sufficient animals compared with respective LPS-treated non-infected controls (Fig. 4a). Thus, infection with a non-lethal pathogen further reduced the overall fitness of Fut2-deficient mice in response to LPS. *C. rodentium* did not induce small intestine IEC fucosylation and did not colonize the small intestine (Extended Data Fig. 8), indicating that systemic challenge by a microbial product was required to reveal the role of inducible fucosylation.

The fitness of infected animals can be maintained through either decreased pathogen burden (resistance), or by an increase in pathogen tolerance without a change in pathogen burden. We quantified the abundance of *C. rodentium* in the faeces of infected mice, as well as the adherence to IECs of *C. rodentium*-expressing luciferase[24,25] (Fig. 4b, c). No differences in pathogen loads were found between Fut2-sufficient and Fut2-deficient animals treated with LPS. Thus, fucosylation of the small intestine upon systemic treatment with LPS probably enhances tolerance of the pathogen. Fut2-negative mice infected with *C. rodentium* and injected with LPS had more pronounced colonic hyperplasia (a trademark of this infection) compared with Fut2-sufficient mice or mice that did not receive LPS (Fig. 4d, e).

Thus, inducible IEC fucosylation might be viewed as an emergency measure taken by the host to support its gut commensals. Fucose used by microbes as an energy source may contribute to protection of the host from endogenous opportunistic pathogens, or it could increase tolerance of infection by regulating bacterial genes responsible for quorum sensing[26] or virulence[27]. Fucose can also serve as a substrate for microbial production of the short-chain fatty acid propionate (Extended Data Fig. 9), which is primarily produced by members of the Bacteroidetes phylum[28]. Whether this process contributes to overall fitness of the animals under infection-induced stress remains to be elucidated. Of note, around 20% of humans lack a functional *FUT2* gene, which is linked to Crohn's disease[29] and to lethality from sepsis in premature infants[30]. Overall, fucosylation of the small intestine in response to systemic microbial exposure can be considered a type of 'tolerance of infection' response. It is interesting, however, that a very similar pathway regulates secretion of antimicrobial

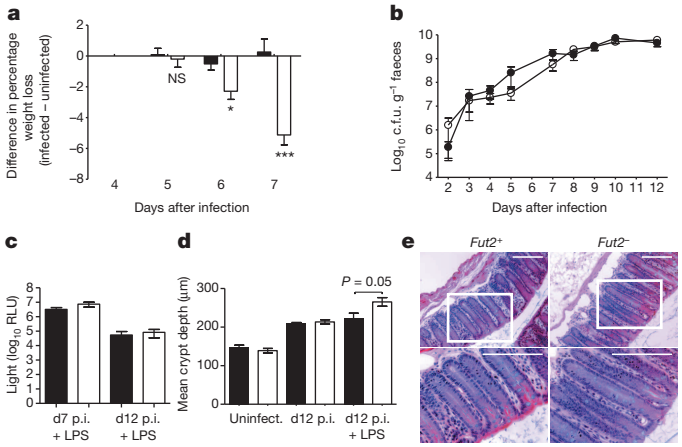

Figure 4 | Host fucosylation increases tolerance of a pathogen. **a**, Difference in percentage weight loss between LPS-injected *C. rodentium*-infected and uninfected mice. Data are shown as mean ± s.e.m.; $*P = 0.01$ $***P = 0.0001$, two-tailed Student's *t* test; combined from six experiments. NS, not significant. **b**, Faecal colony forming units (c.f.u.) of *C. rodentium* from $Fut2^+$ or $Fut2^-$ mice (mean ± s.e.m., representative of three experiments). **c**, Luminescence of thoroughly washed mid-colon of mice infected with *pler-lux*$^+$ *C. rodentium*. $n = 4$ for day (d)12 and 8 for d7; mean ± s.e.m. RLU, relative luminescence units; p.i., post-infection. Data combined from three experiments. **d**, Average crypt depth in uninfected ($n = 3$) or infected mice ($n = 4$) at day 12 post-infection, with or without LPS injection on day 4 post-infection. Data are shown as mean ± s.e.m. (two-tailed Student's *t*-test). In **a**–**d** black bars and circles indicate Fut2-positive mice; open bars and circles indicate Fut2-negative mice. **e**, Representative haematoxylin and eosin staining of distal colon of LPS-treated mice at day 12 after infection. Scale bars = 100 μm. Bottom row shows magnified boxed regions.

proteins—a resistance mechanism[15]. Thus, the mechanisms of resistance and tolerance to pathogens could be evolutionarily linked together to increase the fitness of the host.

Online Content Methods, along with any additional Extended Data display items and Source Data, are available in the online version of the paper; references unique to these sections appear only in the online paper.

Received 16 December 2013; accepted 3 September 2014.
Published online 1 October 2014.

1. Ayres, J. S. & Schneider, D. S. Tolerance of infections. *Annu. Rev. Immunol.* **30,** 271–294 (2012).
2. Ayres, J. S. & Schneider, D. S. The role of anorexia in resistance and tolerance to infections in *Drosophila*. *PLoS Biol.* **7,** e1000150 (2009).
3. Murray, M. J. & Murray, A. B. Anorexia of infection as a mechanism of host defense. *Am. J. Clin. Nutr.* **32,** 593–596 (1979).
4. Kyriazakis, I. I., Tolkamp, B. J. & Hutchings, M. R. Towards a functional explanation for the occurrence of anorexia during parasitic infections. *Anim. Behav.* **56,** 265–274 (1998).
5. Exton, M. S. Infection-induced anorexia: active host defence strategy. *Appetite* **29,** 369–383 (1997).
6. Stecher, B. & Hardt, W. D. Mechanisms controlling pathogen colonization of the gut. *Curr. Opin. Microbiol.* **14,** 82–91 (2011).
7. Bocci, V. & Winzler, R. J. Metabolism of L-fucose-1–^{14}C and of fucose glycoproteins in the rat. *Am. J. Physiol.* **216,** 1337–1342 (1969).
8. Becker, D. J. & Lowe, J. B. Fucose: biosynthesis and biological function in mammals. *Glycobiology* **13,** 41R–53R (2003).
9. Kashyap, P. C. *et al.* Genetically dictated change in host mucus carbohydrate landscape exerts a diet-dependent effect on the gut microbiota. *Proc. Natl Acad. Sci. USA* **110,** 17059–17064 (2013).
10. Ng, K. M. *et al.* Microbiota-liberated host sugars facilitate post-antibiotic expansion of enteric pathogens. *Nature* **502,** 96–99 (2013).
11. Umesaki, Y., Tohyama, K. & Mutai, M. Appearance of fucolipid after conventionalization of germ-free mice. *J. Biochem.* **90,** 559–561 (1981).
12. Bry, L., Falk, P. G., Midtvedt, T. & Gordon, J. I. A model of host-microbial interactions in an open mammalian ecosystem. *Science* **273,** 1380–1383 (1996).
13. Sonnenburg, J. L. *et al.* Glycan foraging *in vivo* by an intestine-adapted bacterial symbiont. *Science* **307,** 1955–1959 (2005).
14. Clark, M. A., Jepson, M. A., Simmons, N. L., Booth, T. A. & Hirst, B. H. Differential expression of lectin-binding sites defines mouse intestinal M-cells. *J. Histochem. Cytochem.* **41,** 1679–1687 (1993).
15. Kinnebrew, M. A. *et al.* Interleukin 23 production by intestinal $CD103^+CD11b^+$ dendritic cells in response to bacterial flagellin enhances mucosal innate immune defense. *Immunity* **36,** 276–287 (2012).
16. Thomsson, K. A. *et al.* Intestinal mucins from cystic fibrosis mice show increased fucosylation due to an induced Fuca1-2 glycosyltransferase. *Biochem. J.* **367,** 609–616 (2002).
17. Holmén, J. M., Olson, F. J., Karlsson, H. & Hansson, G. C. Two glycosylation alterations of mouse intestinal mucins due to infection caused by the parasite *Nippostrongylus brasiliensis*. *Glycoconj. J.* **19,** 67–75 (2002).
18. Domino, S. E., Zhang, L. & Lowe, J. B. Molecular cloning, genomic mapping, and expression of two secretor blood group α (1,2)fucosyltransferase genes differentially regulated in mouse uterine epithelium and gastrointestinal tract. *J. Biol. Chem.* **276,** 23748–23756 (2001).
19. Domino, S. E., Zhang, L., Gillespie, P. J., Saunders, T. L. & Lowe, J. B. Deficiency of reproductive tract α(1,2)fucosylated glycans and normal fertility in mice with targeted deletions of the FUT1 or FUT2 α(1,2)fucosyltransferase locus. *Mol. Cell. Biol.* **21,** 8336–8345 (2001).
20. Vaishnava, S. *et al.* The antibacterial lectin RegIIIγ promotes the spatial segregation of microbiota and host in the intestine. *Science* **334,** 255–258 (2011).
21. Hovel-Miner, G., Faucher, S. P., Charpentier, X. & Shuman, H. A. ArgR-regulated genes are derepressed in the *Legionella*-containing vacuole. *J. Bacteriol.* **192,** 4504–4516 (2010).
22. Zhang, Z., Yen, M. R. & Saier, M. H. Jr. Precise excision of IS5 from the intergenic region between the *fucPIK* and the *fucAO* operons and mutational control of *fucPIK* operon expression in *Escherichia coli*. *J. Bacteriol.* **192,** 2013–2019 (2010).
23. Fischbach, M. A. & Sonnenburg, J. L. Eating for two: how metabolism establishes interspecies interactions in the gut. *Cell Host Microbe* **10,** 336–347 (2011).
24. Kamada, N. *et al.* Regulated virulence controls the ability of a pathogen to compete with the gut microbiota. *Science* **336,** 1325–1329 (2012).
25. Barba, J. *et al.* A positive regulatory loop controls expression of the locus of enterocyte effacement-encoded regulators Ler and GrlA. *J. Bacteriol.* **187,** 7918–7930 (2005).
26. Scott, K. P., Martin, J. C., Campbell, G., Mayer, C. D. & Flint, H. J. Whole-genome transcription profiling reveals genes up-regulated by growth on fucose in the human gut bacterium "*Roseburia inulinivorans*". *J. Bacteriol.* **188,** 4340–4349 (2006).
27. Pacheco, A. R. *et al.* Fucose sensing regulates bacterial intestinal colonization. *Nature* **492,** 113–117 (2012).
28. De Vadder, F. *et al.* Microbiota-generated metabolites promote metabolic benefits via gut-brain neural circuits. *Cell* **156,** 84–96 (2014).
29. McGovern, D. P. *et al.* Fucosyltransferase 2 (FUT2) non-secretor status is associated with Crohn's disease. *Hum. Mol. Genet.* **19,** 3468–3476 (2010).
30. Morrow, A. L. *et al.* Fucosyltransferase 2 non-secretor and low secretor status predicts severe outcomes in premature infants. *J. Pediatr.* **158,** 745–751 (2011).

Supplementary Information is available in the online version of the paper.

Acknowledgements We thank C. Reardon and C. Daly for sequencing support, H. Ye for help with metabolic cage analysis, N. F. Dalleska for assistance and use of GC–MS instrumentation in the Environmental Analysis Center at the California Institute of Technology, and G. Nuñez for luciferase-expressing *C. rodentium*. This work was supported by grants from the National Institutes of Health (P50 GM068763 to P.J.T., AI96706 and AI42135 to E.G.P., T32 AI065382 to J.M.P.), the Harvard Bauer Fellows Program, National Science Foundation grant EFRI-1137089 to R.F.I. and A.V.C., Digestive Disease Research Core Center grant DK42086 and a Kenneth Rainin Foundation grant to A.V.C.

Author Contributions J.M.P., M.A.K., M.C.A. and E.G.P. performed analysis of inducible fucosylation in mice, including mutant strains; J.M.P. and C.F.M. produced DNA and RNA sequencing data and P.J.T. analysed these data; D.S. produced *Myd88*$^{fl/fl}$ mice; T.V.G. produced GF BALB/c mice and performed cytokine ELISA analysis; S.R.B. and R.F.I. performed analysis of short-chain fatty acids; R.F.I., E.G.P. and P.J.T. contributed to writing of the manuscript; A.V.C. conceived the project, analysed the results and wrote the manuscript. All authors discussed the results and commented on the manuscript.

Author Information The DNA and RNA shotgun sequencing data have been deposited in the Gene Expression Omnibus database under accession number GSE60874; 16S rRNA gene sequencing reads have been deposited in MG-RAST under accession number 10494. Reprints and permissions information is available at www.nature.com/reprints. The authors declare no competing financial interests. Readers are welcome to comment on the online version of the paper. Correspondence and requests for materials should be addressed to A.V.C. (achervon@bsd.uchicago.edu).

METHODS

Mice. BALB/cJ, C57BL/6J, NOD/LtJ, C3H/HeN, *Rag1*$^{-/-}$ (B6.129S7-Rag1^{tm1Mom}/J), *Fut2*$^{-/-}$ (B6.129X1-Fut2^{tm1Sdo}/J), Villin-Cre (B6.SJL-Tg(Vil-Cre)997Gum/J), and CD11c-Cre (C57BL/6J-Tg(Itgax-Cre,-EGFP)4097Ach/J) mice were purchased from The Jackson Laboratory. *Fut2*$^{-/-}$ mice were backcrossed greater than seven generations to BALB/c. Knockout mice produced litters of mixed genotypes kept co-housed to homogenize their gut microbiota. B6 *Myd88*$^{-/-}$ mice were a gift from S. Akira. B6 MyD88 floxed mice were described previously[31]. *Rorc*$^{-/-}$ (ref. 32), and *IL23p19*$^{-/-}$ (also known as *Il23a*$^{-/-}$)[33] mice were provided by Y.-X. Fu. *Il22*$^{-/-}$ mice[34] were maintained at the Memorial Sloan-Kettering Cancer Center. Mice were housed in a specific pathogen-free facility and used in accordance with institutional guidelines for animal welfare. Six- to twelve-week-old male and female mice were used for randomization purposes. The numbers of mice per group were chosen as the minimum needed to obtain biologically significant results, based on previous experience. Evaluations were made in a blind fashion. Functional experiments were done with Fut2-negative mice on the BALB/c genetic background using Fut2-sufficient littermates as controls.

Metabolic studies. Mice were single-housed in TSE Systems LabMaster cages to monitor physical activity (*x*/*y* and *z* axes by infrared beams crossed), drinking and feeding.

Fucosylation activation *in vivo*. LPS from *S. enterica* ssp. Typhimurium (#L6511, Sigma-Aldrich) was injected i.p. at 1 μg g^{-1} body weight, or gavaged to GF mice at 1 mg in 400 μl sterile PBS. CpG (100 μg CpG-B ODN 1826, Coley Pharmaceutical Group) and Pam_3CSK_4 (100 μg, Invivogen), were injected i.p. Carrier-free recombinant mouse IL-22 (Biolegend,) was diluted in 1% BSA/PBS and 1.5 μg was given i.p.

Antibiotic treatment. Ampicillin (1 g l^{-1}) and 200 mg l^{-1} vancomycin (Sigma-Aldrich) were 0.22 μm filtered and added to autoclaved drinking water starting 2 days before LPS treatment (day −2) and lasting for the duration of the experiment.

Lectin staining. For whole-mount staining, small intestine was removed, a 1 cm piece from the upper third was excised, opened, cleaned of mucus in cold PBS, and incubated with *Ulex europaeus* agglutinin-1 (UEA-1) conjugated to FITC, TRITC or atto-594 (Vector Laboratories or Sigma-Aldrich) for 15 min on ice. Tissue was placed lumen side up on a slide for microscopy. For *Il22*$^{-/-}$ experiments, whole tissue was fixed in 4% paraformaldehyde before proceeding with whole-mount staining. Fixation did not affect staining pattern or intensity.

For staining of sections, tissues were fixed in 2% paraformaldehyde overnight at 4 °C, cryoprotected in 20% sucrose/PBS overnight at 4 °C, and embedded in OCT compound (Sakura Finetek), and 10 μm sections were stained with UEA-1–FITC (1 μg ml^{-1}, Vector) for 30 min at room temperature, and incubated for 20 min at 37 °C in propidium iodide (0.5 μg ml^{-1}, Sigma-Aldrich) with RNase A (10 μg ml^{-1}, Sigma-Aldrich) to label nuclei.

For single-cell analysis by FACS, small intestine (with Peyer's patches and mesenteric fat removed) was divided into equal thirds, opened longitudinally and washed with cold PBS. Tissue was cut into 1 cm pieces and shaken in 10 mM EDTA/1 mM dithiothreitol (DTT)/PBS at 37 °C for 20 min, and filtered through nylon mesh. Single-cell suspensions were pelleted and fixed in 5 ml of 1% paraformaldehyde overnight at room temperature. Cells were then stained with UEA-1–FITC (1 μg ml^{-1}, Vector), and gated on the FSC/SSC high epithelial cell population.

Light microscopy. Fluorescence microscopy of whole-mounts and sections used a Leica DM LB microscope (Leica Camera AG) and Spot RT Slider camera and software (Diagnostic Instruments). Confocal microscopy of bacteria was performed with an Olympus DSU spinning disk microscope and Slidebook software (3I). All images in an experiment were taken using the same exposure settings.

Scanning electron microscopy. Tissues were fixed in 2% paraformaldehyde/2% glutaraldehyde/0.1 M cacodylate buffer, transferred to cacodylate buffer overnight and processed with the OTOTO procedure[35]. To dehydrate, samples were passed through increasing concentrations of acetone in water, followed by hexamethyldisilazane (Electron Microscopy Sciences). Samples were mounted with colloidal silver paste (Electron Microscopy Sciences) and imaged with an FEI Nova NanoSEM 230 (FEI) at 5 kV.

Identification of fucosylated proteins. To visualize fucosylated proteins in the lumen contents, the intestinal contents were gently removed by squeezing and homogenized at 1 g sample per 5 ml of Tris-Triton-X-100 buffer (150 mM NaCl, 50 mM Tris pH 8, 1% Triton X-100, and protease inhibitor tablet (Roche)) on ice and spun at 17,000*g* for 20 min at 4 °C. Supernatant proteins were separated by 6% non-reducing SDS–PAGE, transferred to PVDF membrane (Bio-Rad), blocked with 0.5% gelatin in 0.05% Tween-20/PBS, and visualized with UEA-1–HRP (1 μg ml^{-1}, Sigma-Aldrich).

For sequencing of fucosylated epithelial cell proteins, small intestine epithelial cells were isolated as described earlier and lysed in Tris-Triton-X-100 buffer. Lysates were pre-cleared by incubating with unconjugated agarose beads (Vector) twice for 45 min at 4 °C. Cleared lysates were then incubated with washed UEA-1-conjugated beads (Vector) for 45 min. Beads were washed five times to remove unbound protein. To elute UEA-1-bound protein, beads were incubated with 200 mM L-fucose (Sigma-Aldrich) for 30 min. Eluted proteins were separated on a 4–15% gradient SDS–PAGE gel (Bio-Rad), silver-stained (Thermo Fisher Scientific), and bands were excised for identification by mass spectrometry at the Taplin Biological Mass Spectrometry Facility, Harvard Medical School.

Isolation of fucosidase-positive bacteria. Brain heart infusion (BHIS) agar plates (Becton, Dickinson, and Co.) with added thioglycolic acid, menadione and hematin/histidine (Sigma-Aldrich) were pre-reduced in an anaerobic chamber with 2.5% hydrogen atmosphere at 37 °C, and spread with 40 μl of 5-bromo-4-chloro-3-indolyl-α-L-fucopyranoside (50 mM in DMF) (Carbosynth). Faecal pellets were homogenized in reduced 0.01% thioglycolic acid/PBS, plated, and grown for 3 days at 37 °C anaerobically, then at 4 °C aerobically to develop colour. Blue colonies were identified by sequencing of their 16S rDNA genes using primers 8F (5′-AGAGTTTGATCCTGGCTCAG-3′) and 1391R (5′-GACGGGCGGTGWGTRCA-3′), and sequencing of their *gyrB* genes using primers gyrB F (5′-GAAGTCATCATGACCGTTCTGCAYGCNGGNGGNAARTTYGA-3′) and gyrB R (5′-AGCAGGGTACGGATGTGCGAGCCRTCNACRTCNGCRTCNGTCAT-3′) for amplification and gyrB FS (5′-GAAGTCATCATGACCGTTCTGCA-3′) and gyrB RS (5′-AGCAGGGTACGGATGTGCGAGCC-3′) for sequencing[36]. *B. thetaiotaomicron* VPI-5482 and *B. uniformis* (a gift from C. Nagler) were used as controls.

Measurement and inhibition of fucosidase activity. Faecal pellets were weighed and homogenized in 10 μl PBS per 1 mg sample, and centrifuged at 17,000*g* for 10 min. Fifty microlitres of this supernatant was incubated for 1 h at 37 °C with or without adding 0.5 μl of 50 mM 4-methylumbelliferyl fucopyranoside (in dimethylsulphoxide (DMSO), Sigma or Gold Biotechnology). The reaction was diluted 100-fold in 0.2 M glycine-NaOH buffer, pH 10.5, and fluorescence was measured at 365 nm excitation, 445 nm emission. Fluorescence of the no-substrate control was subtracted from the substrate-containing reaction. The amount of cleaved substrate and fucosidase activity was then calculated by comparison to a standard curve of 4-methylumbelliferone (Sigma) in glycine-NaOH buffer. Deoxyfuconojirimycin (DFJ; Enzo Life Sciences) was dissolved in PBS and gavaged to mice in 100 μl (5 μmol total).

Reporter *E. coli*. The pXDC94 plasmid[21], containing the ptac promoter controlling mCherry expression and a multiple cloning site upstream of the promoter-less *GFP* gene, was a gift from H. Shuman. The promoter region upstream of the *E. coli fucPIK* genes[22] was amplified using primers that added restriction sites (bold) at the 5′ and 3′ ends of the amplicon, respectively: fucproF, 5′-TAT**GGTACC**GGATTCATTTTCAAATAAAA-3′; fucproR, 5′-TAT**CCCGGG**TAGCTACCTCTCTCTGATTC-3′. The PCR product and vector were digested with XmaI and KpnI (New England Biolabs), gel purified, ligated, and introduced into *E. coli* K-12 strain BW25113 (Yale Coli Genetic Stock Center) by electroporation. Correct expression of mCherry and GFP was verified by growth in minimal medium[37] with 10 mM glucose and the indicated concentrations of fucose.

E. coli K12 bacteria carrying the pXDC94-fucPIK-pro reporter were grown overnight in Luria–Bertani broth (LB) with shaking at 37 °C, centrifuged at 5,000*g*, resuspended to ~10^9 c.f.u. ml^{-1} in PBS, and 400 μl gavaged to mice that had received LPS i.p. 6 h earlier (SPF mice), or at the time of gavage (gnotobiotic mice). For dual colonization with *B. acidifaciens*, 100 μl of stationary-phase culture was gavaged at the same time as *E. coli*. Twenty-four hours after gavage, mice were killed and their caecum and colon contents were homogenized in PBS. Bacteria were enriched by centrifuging at 200*g* for 5 min, centrifuging the supernatant at 5,000*g* for 5 min, and resuspending the pellet in 750 μl PBS. This was underlain with 300 μl Histopaque-1119 (Sigma-Aldrich) and centrifuged for 1 min at 11,600*g*. The interface containing mostly bacteria was washed with PBS, fixed in 2% paraformaldehyde for 20 min at room temperature, washed and resuspended in 50–100 μl PBS. Four microlitres of bacterial suspension was placed on a slide and coverslipped. Random fields were selected using red fluorescence only, and an image was acquired in both the red and green channels. Fluorescence of individual bacteria were measured in ImageJ 1.41 software[38] by gating on areas of red fluorescence and measuring the mean green pixel intensity within the gated area.

Estimation of total bacterial loads. Fresh faecal pellets were placed in an anaerobic chamber and mashed in 500 μl of reduced PBS containing 0.01% thioglycolic acid. Serial dilutions were made in reduced PBS and plated on pre-reduced Brucella blood agar plates (Becton, Dickinson, and Co.; for anaerobic counts), removed from the anaerobic chamber, and plated on tryptic soy agar (TSA)/5% sheep's blood plates (Becton, Dickinson, and Co.; aerobic counts). Total colonies were counted after 2 days (aerobic) or 3 days (anaerobic) incubation at 37 °C.

For 16S copy number, faecal pellets were weighed, DNA was isolated by a bead beating and phenol/chloroform extraction method[39], and qPCR performed and copy number determined as described[40].

***S. enterica* Typhimurium and *C. rodentium* infection.** For *S. enterica* Typhimurium infection, mice were gavaged with 20 mg streptomycin (Sigma) in 100 μl sterile

water, 24 h before infection. *S. enterica* Typhimurium strain SL1344 was grown overnight in LB with streptomycin (50 μg ml^{-1}) and gavaged to mice at 5×10^8 c.f.u. in 100 μl volume.

C. rodentium strains DBS100 or DBS120 p*ler-lux* were grown in LB overnight at 37 °C, then diluted 1:100 and grown for 2.5 h, centrifuged and resuspended in 0.01 volumes PBS, and mice were gavaged with ~5×10^9 bacteria in 100 μl LB. To determine mouse colonization levels, a fresh faecal pellet or small intestine contents (gently squeezed to remove, except last 3 cm of ileum) was weighed, mashed in 500 μl of PBS, serially diluted, and plated on MacConkey (Becton, Dickinson, and Co.) or LB agar with 50 μg ml^{-1} kanamycin. For luciferase measurements, the faecal homogenate was adjusted to 10 mg in 1 ml PBS in an Eppendorf tube and light measured in a Triathler scintillation counter (Hidex), before plating dilutions in PBS on agar with kanamycin. Colon-adherent bacteria were measured in a 1 cm piece from the middle of the colon. The piece was opened longitudinally, washed in 1 mM DTT/PBS by vortexing for 10 s, then washed in PBS, and placed in an Eppendorf in 500 μl PBS for light measurement as before. The piece was then mashed and dilutions plated on agar with kanamycin.

Histology. Distal colon from *C. rodentium*-infected mice or uninfected controls was fixed in neutral formalin, then kept in 70% EtOH until being embedded in paraffin, and 5 μm sections were cut and stained with haematoxylin and eosin. Well-oriented crypts were photographed and their lengths measured in ImageJ, and the mean taken for each mouse.

Serum cytokine ELISA. Serum concentrations were measured by ELISA according to the manufacturer's instructions (IL-1β: eBioscience; IL-6 and TNF-α: Becton, Dickinson and Co.).

Short-chain fatty acid measurements. For gavage experiments, food was removed and SPF mice were gavaged at 0, 3 and 6 h with 300 μl of 0.1 M L-fucose or 0.1 M D-galactose (Sigma-Aldrich) in autoclaved tap water, or water only. At 8 h, mice were killed and caecal contents removed and kept at −80 °C until processing.

Concentrations of the short-chain fatty acids in caecal contents were measured using the direct injection gas chromatography–mass spectrometry (GC–MS) method adapted from that described previously[41–43].

Caecal contents were extracted in two steps. Deionized water was added to the samples at the amount of 5 ml per 1 g of sample, followed by brief vortex-mixing and sonication for 15 min. In the second step, acetonitrile (#1103, BDH) containing 20 mM of tetradeuteroacetic acid (#16621, Acros Organics) was added to the aqueous extracts at the amount of 5 ml per 1 g of initial sample, followed by the second round of brief vortex-mixing and sonication for 15 min.

Extracted samples were centrifuged for 5 min at 17,000*g* and 0.02 ml of clear supernatant was mixed with 0.98 ml of acetonitrile containing 20 mM of formic acid (#94318, Fluka) and 0.05 mM of 2-ethylbutyric acid (#109959, Aldrich). The mixtures were briefly vortex-mixed and centrifuged for 5 min at 17,000*g* and 1 μl of the obtained supernatants were analysed by direct injection GC–MS on an Agilent 6890N GC system equipped with a Mass Selective (MS) Detector 5973 (Agilent Technologies).

The instrument was used in a splitless mode with an installed double taper inlet liner (#23308, Sky by Restek) and fused-silica column with polyethylene glycol stationary phase (INNOWax #19091N-133, J&W Scientific, Agilent Technologies) 30 m × 0.25 mm ID coated with 0.25 μm film.

Helium carrier gas was supplied at 1.00 ml min^{-1} flow rate. The injection port temperature was 260 °C. The initial oven temperature of 60 °C was maintained for 2 min, then increased to 150 °C at 10 °C min^{-1} and further to 250 °C at 25 °C min^{-1} and held at that temperature for 4 min, bringing the total duration of the run to 19 min. The MS detector temperature was set to 245 °C.

GC–MS data were analysed using the MSD ChemStation D.01.02.16 software (Agilent Technologies). Tetradeuteroacetic and 2-ethylbutyric acids served as internal standards.

Enzymatic activity of digestive enzymes. Epithelial cells were dissociated from the upper half of the small intestine as described earlier. Haematopoietic cells were removed with anti-CD45-biotin (clone 30-F11, Biolegend) and streptavidin magnetic beads with a MACS LS column (Miltenyi Biotec). Epithelial cells were diluted in 96-well plates in triplicate in appropriate substrate solutions (for sucrase, 60 mM sucrose in PBS; for maltase, 30 mM maltose in PBS; for aminopeptidase, 5 mM leu-pNA (Enzo Life Sciences) in 50 mM TRIS, pH 7.4). Cells were incubated for 30–60 min at 37 °C. For the aminopeptidase assay, absorbance was measured at 405 nm. For the sucrase and maltase assays, plates were centrifuged and 5 μl of supernatant was used for a colorimetric assay to measure liberated glucose (Cayman Chemical).

Metagenomic library preparation and sequencing. Methods for microbial community DNA and mRNA sequencing were as previously described[44,45]. Faecal pellets collected from mice before or after LPS treatment (pooled from 2 and 3 days post-injection) were kept at −80 °C until DNA and RNA isolation using the guanidinium thiocyanate/caesium chloride gradient method[46] as described, except that crude particles were removed by centrifugation before overlaying the gradient. RNA was subjected to DNase treatment (Ambion), purification using MEGAClear columns (Ambion), and rRNA depletion via subtractive hybridization (MICROBExpress, Ambion, in addition to custom depletion oligonucleotides). The presence of genomic DNA contamination was assessed by PCR with universal 16S rDNA primers. cDNA was synthesized using SuperScript II and random hexamers (Invitrogen), followed by second-strand synthesis with RNaseH and *E.coli* DNA polymerase (New England Biolabs). Samples were prepared for sequencing with an Illumina HiSeq instrument after enzymatic fragmentation (NEBE6040L/M0348S). Libraries were quantified by qPCR according to the Illumina protocol. qPCR assays were run using ABsoluteTM QPCR SYBR Green ROX Mix (Thermo Scientific) on an Mx3000P QPCR System instrument (Stratagene). The size distribution of each library was quantified on an Agilent HS-DNA chip (Agilent).

16S rRNA gene sequencing and analysis. Community DNA was PCR-amplified using universal bacterial primers targeting variable region 4 of the 16S rRNA gene with the following thermocycler protocol: denature at 94 °C for 3 min, 35 cycles of 94 °C for 45 s, 50 °C for 30 s, and 72 °C for 90 s, with a final extension at 72 °C for 10 min[45,47,48]. Triplicate reactions for each sample were pooled and amplification was confirmed by 1.5% gel electrophoresis. 16S rRNA gene amplicons were cleaned with the Ampure XP kit (Agencourt) and quantified using the Quant-iT Picogreen ds DNA Assay Kit (Invitrogen). Barcoded amplicons from multiple samples were pooled and sequenced using the Illumina HiSeq platform[47]. 16S rRNA gene sequences were analysed using the QIIME (Quantitative Insights Into Microbial Ecology)[44] software package along with custom Perl scripts. Data sets were randomly subsampled before clustering analyses at a depth that retained all of the individual samples (180,000 sequences per sample). All sequences were used for the comparison of the relative abundance of bacterial taxonomic groups. OTUs were picked at 97% similarity against the Greengenes database[49] (constructed by the nested_gg_workflow.py QiimeUtils script on 4 February 2011), which we trimmed to span only the 16S rRNA region flanked by our sequencing primers (positions 521–773). The LefSe package was used to identify taxonomic groups significantly associated with each treatment[50]. LefSe was run on the sub-sampled data sets, after filtering out species-level OTUs with <100 sequences or present in only 1 sample. Statistical analyses were also performed using the QIIME scripts 'otu_category_significance' (ANOVA) and 'compare_categories.py' (PERMANOVA).

Reference genome database. A custom database was constructed from draft and finished reference genomes obtained from human-associated microbial isolates (538 genomes from the Human Microbiome Project Data Analysis and Coordination Center (http://www.hmpdacc.org)), in addition to the *Eggerthella lenta* DSM2243 reference genome. All predicted proteins from the reference genome database were annotated with KEGG orthologous groups (KOs) using the KEGG database (version 52; BLASTX *e*-value < 10^{-5}, bit score > 50, and >50% identity)[51]. For query genes with multiple matches, the annotated reference gene with the lowest *e*-value was used. When multiple annotated genes with an identical *e*-value were encountered after a BLAST query, we included all KOs assigned to those genes. Genes from the database with significant homology (BLASTN *e*-value < 10^{-20}) to non-coding transcripts from the 539 microbial genomes were excluded from subsequent analysis.

Metagenomic sequence analysis. DNA- and RNA-seq analysis was performed with our recently described pipeline[45]. Briefly, high-quality reads (see Supplementary Table 1 for sequencing statistics) were mapped using SSAHA2[52] to our custom 539-genome database and the Illumina adaptor sequences (SSAHA2 parameters: '-best 1 -score 20 –solexa'). The number of transcripts assigned to each gene was then tallied and normalized to reads per kilobase per million mapped reads (RPKM). To account for genes that were not detected owing to limited sequencing depth, a pseudocount of 0.01 was added to all samples. Samples were clustered in Matlab (version 7.10.0) based on gene expression or abundance. Genes were grouped by KOs by calculating the cumulative RPKM for each sample for genes present in at least six samples. We used HUMAnN, a recently developed software package for metabolic reconstruction from metagenomic data[53], followed by LefSe analysis to identify metagenomic biomarkers[50]. A modified version of the "SConstruct" file was used to input KO counts into the HUMAnN pipeline for each RNA-seq data set. We then ran LefSe on the resulting KEGG module abundance file using the '-o 1000000' flag. We used the edgeR package[54] to identify orthologous groups with significantly altered abundance or expression. Prior to analysis, we calculated the cumulative number of sequencing reads assigned to each sample for each KO (without RPKM normalization). We then used a paired glm analysis to determine consistent changes within each animal following LPS treatment. Default parameters were used, with one exception: for the estimateGLMTrendedDisp step 'min.n' was set to 50/300 for the genomes and KO, respectively. Significance was accepted at a false discovery rate (FDR) < 0.05 and >2-fold change.

PCR and RT–PCR. RNA was isolated from mouse tissues and gut contents by the guanidinium thiocyanate/caesium chloride gradient method[46]. RNA was DNase treated (Sigma) and reverse transcribed with Superscript III (Invitrogen). Primer sequences were as follows: fut1F, 5′-CAAGGAGCTCAGCTATGTGG-3′, fut1R, 5′- GACTGCTCAGGACAGGAAGG-3′; fut2F, 5′-ACAGCCAGAAGAGCCAT

GGC-3′, fut2R, 5′-TAACACCGGGAGACTGATCC-3′; sec1F, 5′-ATCCAAGC AGTGCTCCAGC-3′, sec1R, 5′-CAATATTCGCCCATCTGGTTC-3′; villinF, 5′-G CTTGCCACAACTTCCTAAG-3′, villinR, 5′-CTTGCTTGAAGTAGCTCCGG-3′. Quantitative RT–PCR was performed on an Applied Biosystems StepOnePlus instrument with Universal Sybr Green Universal Supermix (Bio-Rad), and the following primers[27]: *E. coli* fucA F, 5′-GGCGCGCAAGGAATAGAA-3′, *E. coli* fucA R, 5′-GATCCCCGCTATTCACTACATGA-3′; *E. coli* fucP F, 5′-CCAAATACGGTTC GTCCTTCA-3′, *E. coli* fucP R, 5′-ACCCATGACCGGAGTGACAA-3′; *E. coli* rpoA F, 5′-GCGCTCATCTTCTTCCGAAT-3′, *E. coli* rpoA R, 5′-CGCGGTCGTGGT TATGTG-3′.

Statistics. Statistical analyses were performed with GraphPad Prism 5 software (GraphPad Software).

31. Kleinridders, A. *et al.* MyD88 signaling in the CNS is required for development of fatty acid-induced leptin resistance and diet-induced obesity. *Cell Metab.* **10,** 249–259 (2009).
32. Eberl, G. *et al.* An essential function for the nuclear receptor RORγt in the generation of fetal lymphoid tissue inducer cells. *Nature Immunol.* **5,** 64–73 (2004).
33. Cua, D. J. *et al.* Interleukin-23 rather than interleukin-12 is the critical cytokine for autoimmune inflammation of the brain. *Nature* **421,** 744–748 (2003).
34. Zenewicz, L. A. *et al.* Interleukin-22 but not interleukin-17 provides protection to hepatocytes during acute liver inflammation. *Immunity* **27,** 647–659 (2007).
35. Malick, L. E. & Wilson, R. B. Modified thiocarbohydrazide procedure for scanning electron microscopy: routine use for normal, pathological, or experimental tissues. *Stain Technol.* **50,** 265–269 (1975).
36. Sakamoto, M. & Ohkuma, M. Identification and classification of the genus *Bacteroides* by multilocus sequence analysis. *Microbiology* **157,** 3388–3397 (2011).
37. Boronat, A. & Aguilar, J. Rhamnose-induced propanediol oxidoreductase in *Escherichia coli*: purification, properties, and comparison with the fucose-induced enzyme. *J. Bacteriol.* **140,** 320–326 (1979).
38. Schneider, C. A., Rasband, W. S. & Eliceiri, K. W. NIH Image to ImageJ: 25 years of image analysis. *Nature Methods* **9,** 671–675 (2012).
39. Ubeda, C. *et al.* Vancomycin-resistant *Enterococcus* domination of intestinal microbiota is enabled by antibiotic treatment in mice and precedes bloodstream invasion in humans. *J. Clin. Invest.* **120,** 4332–4341 (2010).
40. Buffie, C. G. *et al.* Profound alterations of intestinal microbiota following a single dose of clindamycin results in sustained susceptibility to *Clostridium difficile*-induced colitis. *Infect. Immun.* **80,** 62–73 (2012).
41. Fleming, S. E., Traitler, H. & Koellreuter, B. Analysis of volatile fatty acids in biological specimens by capillary column gas chromatography. *Lipids* **22,** 195–200 (1987).
42. Tangerman, A. & Nagengast, F. M. A gas chromatographic analysis of fecal short-chain fatty acids, using the direct injection method. *Anal. Biochem.* **236,** 1–8 (1996).
43. Zhao, G., Nyman, M. & Jonsson, J. A. Rapid determination of short-chain fatty acids in colonic contents and faeces of humans and rats by acidified water-extraction and direct-injection gas chromatography. *Biomed. Chromatogr.* **20,** 674–682 (2006).
44. Caporaso, J. G. *et al.* QIIME allows analysis of high-throughput community sequencing data. *Nature Methods* **7,** 335–336 (2010).
45. Maurice, C. F., Haiser, H. J. & Turnbaugh, P. J. Xenobiotics shape the physiology and gene expression of the active human gut microbiome. *Cell* **152,** 39–50 (2013).
46. Chirgwin, J. M., Przybyla, A. E., MacDonald, R. J. & Rutter, W. J. Isolation of biologically active ribonucleic acid from sources enriched in ribonuclease. *Biochemistry* **18,** 5294–5299 (1979).
47. Caporaso, J. G. *et al.* Ultra-high-throughput microbial community analysis on the Illumina HiSeq and MiSeq platforms. *ISME J.* **6,** 1621–1624 (2012).
48. Caporaso, J. G. *et al.* Global patterns of 16S rRNA diversity at a depth of millions of sequences per sample. *Proc. Natl Acad. Sci. USA* **108** (suppl. 1), 4516–4522 (2011).
49. DeSantis, T. Z. *et al.* Greengenes, a chimera-checked 16S rRNA gene database and workbench compatible with ARB. *Appl. Environ. Microbiol.* **72,** 5069–5072 (2006).
50. Segata, N. *et al.* Metagenomic biomarker discovery and explanation. *Genome Biol.* **12,** R60 (2011).
51. Kanehisa, M., Goto, S., Kawashima, S., Okuno, Y. & Hattori, M. The KEGG resource for deciphering the genome. *Nucleic Acids Res.* **32,** D277–D280 (2004).
52. Ning, Z., Cox, A. J. & Mullikin, J. C. SSAHA: a fast search method for large DNA databases. *Genome Res.* **11,** 1725–1729 (2001).
53. Abubucker, S. *et al.* Metabolic reconstruction for metagenomic data and its application to the human microbiome. *PLoS Comput. Biol.* **8,** e1002358 (2012).
54. Robinson, M. D., McCarthy, D. J. & Smyth, G. K. edgeR: a Bioconductor package for differential expression analysis of digital gene expression data. *Bioinformatics* **26,** 139–140 (2010).

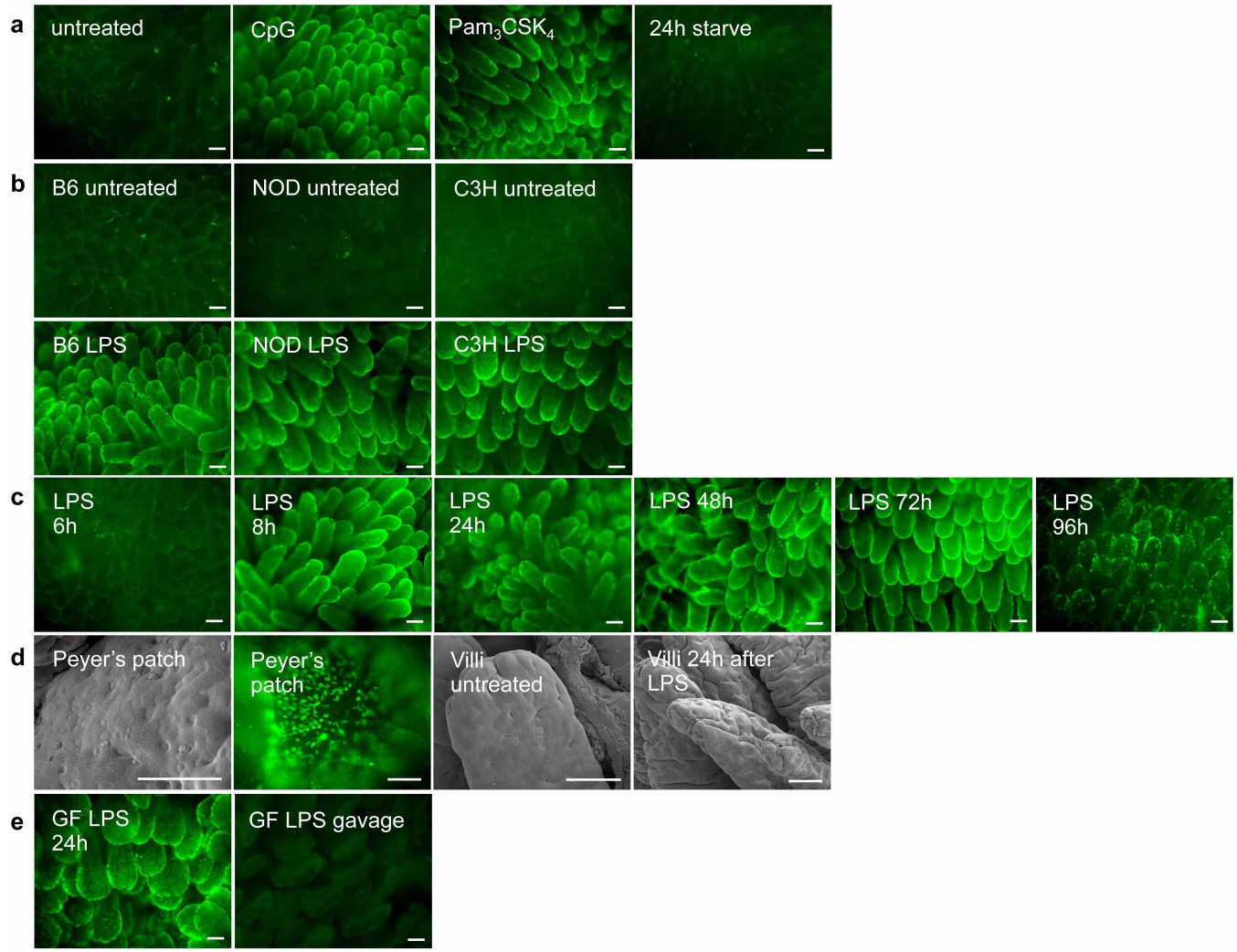

Extended Data Figure 1 | Requirements and kinetics for small intestine fucosylation induced by systemic injection of TLR ligands. **a**, Systemic injection of bacterial TLR ligands induces small intestine fucosylation, but simple starvation does not. UEA-1 staining (as in Fig. 1) after i.p. injection of CpG DNA, or Pam_3CSK_4, or food deprivation for 24 h of BALB/c SPF mouse. **b**, LPS injection causes small intestine fucosylation in various inbred mouse strains. SPF mice of the indicated strains were injected with LPS i.p. and the small intestine was stained with UEA-1 after 24 h, as in Fig. 1. **c**, Fucosylation peaks at 8 h after LPS injection and is still detectable at 96 h. **d**, M cells can be readily detected by scanning electron microscope and UEA-1 staining of the domes of the Peyer's patches, but are rare in the villi and are not massively induced in the villi by LPS injection. UEA-1 staining and scanning electron microscopy were performed on adjacent pieces from the proximal one-third of the small intestine. Scale bars = 100 μm for UEA-1 staining, 50 μm for scanning electron microscope images. **e**, Small intestine fucosylation does not require the presence of endogenous microbiota (LPS injection in GF mouse) and is not induced by oral administration of LPS (1 mg). All data are representative of at least two independent experiments.

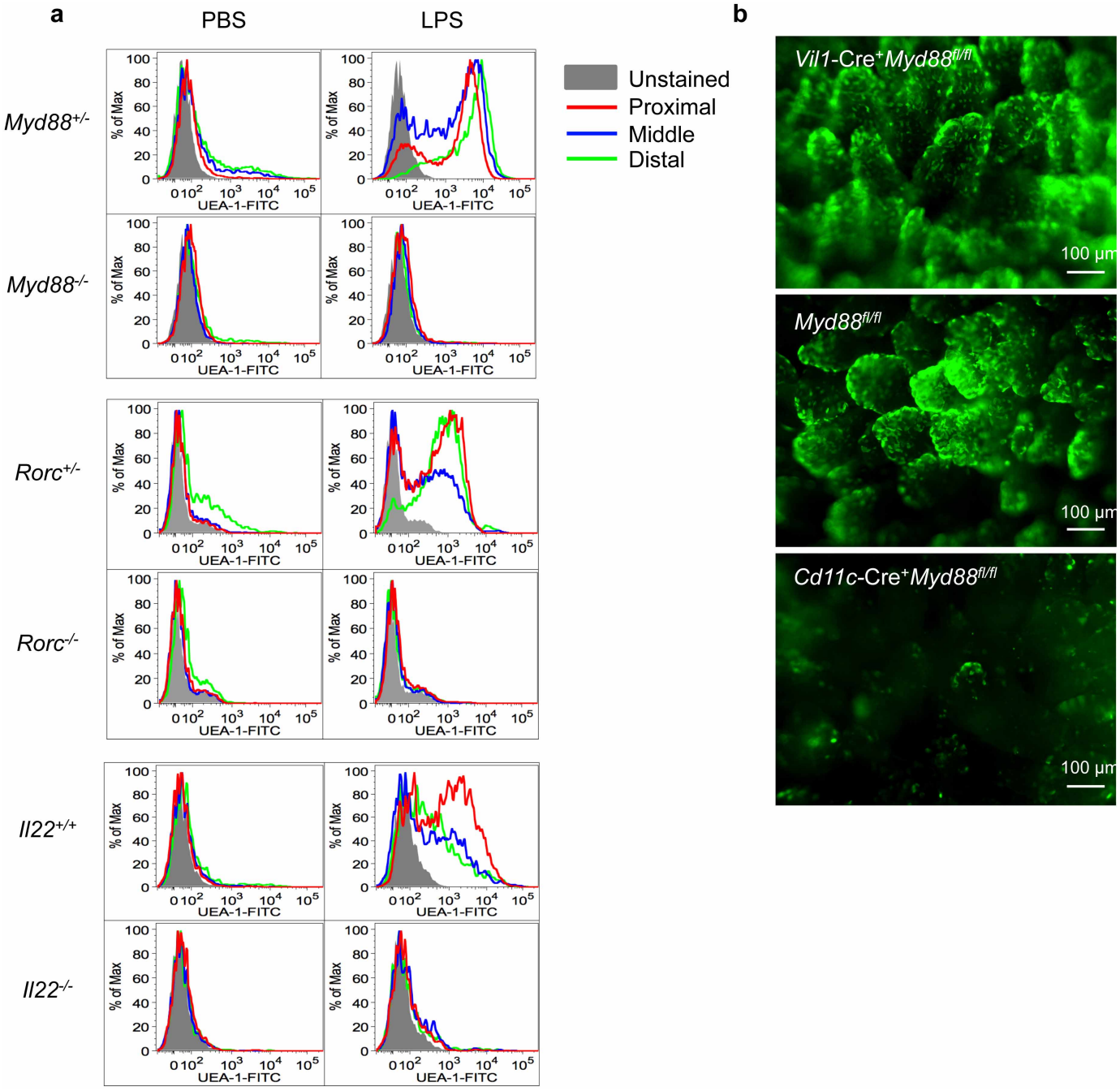

Extended Data Figure 2 | MyD88-dependent pathway for fucosylation of small intestine IECs in response to systemic stimulation of TLRs. a, FACS analysis of IECs from three segments of small intestine from the indicated mice. Cells are gated on the FSC/SSC high epithelial cell population. At least two mice per mutant genotype were stained along with two control mice in the experiments shown. **b**, SPF mice were pre-treated with 20 mg streptomycin and orally infected with *S. enterica* Typhimurium. The small intestine was stained at 24 h post-infection. MyD88 expression was necessary in $CD11c^+$ cells but not $villin^+$ IECs for *S. enterica* Typhimurium-induced fucosylation. Data are representative of at least two independent experiments.

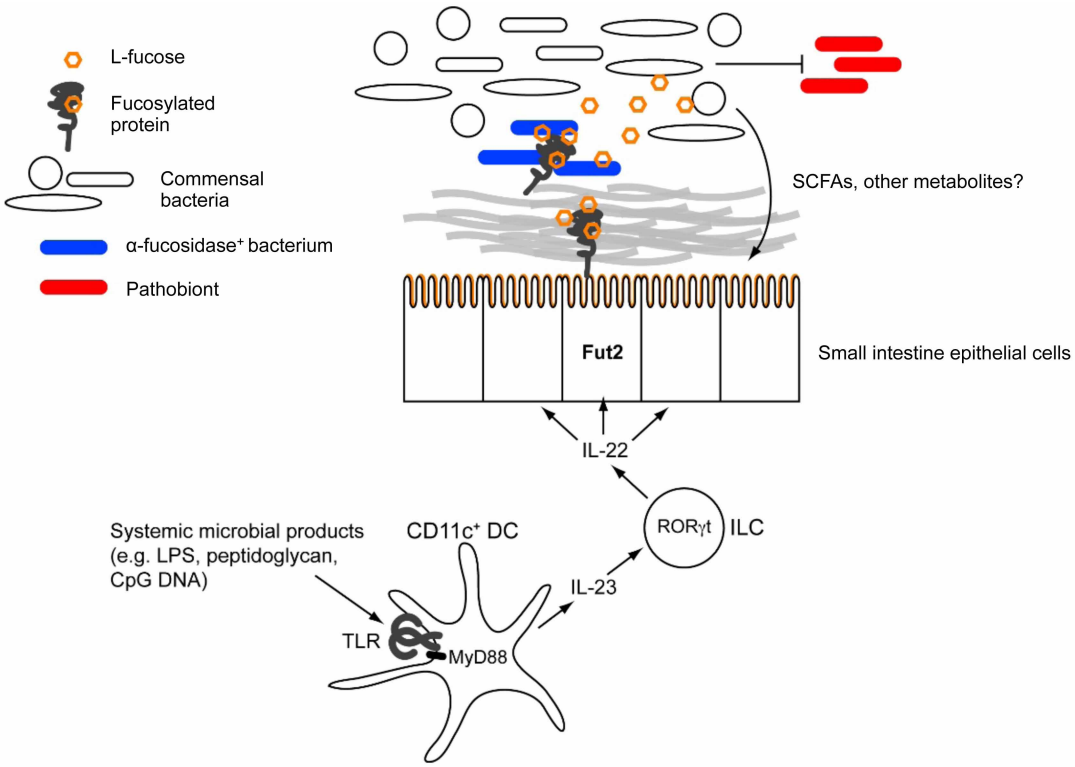

Extended Data Figure 3 | A proposed model for the mechanisms linking inducible fucosylation to the gut microbiota. Systemic microbial agonists activate TLRs on $CD11c^{+}$ dendritic cells (DCs), causing secretion of the cytokine IL-23, which in turn stimulates RORγt-dependent ILCs to secrete IL-22. IL-22 causes small intestine epithelial cells to upregulate Fut2. Fucosylated proteins are either secreted into the lumen or expressed on the cell surface and later shed into the lumen. Fucosidase-expressing bacteria (blue) liberate fucose residues, which they can utilize and share with other bacteria lacking the fucose-cleaving enzyme. Bacterial metabolism of fucose potentially produces metabolites such as short-chain fatty acids (SCFAs). Fucose also directly or indirectly downregulates virulence gene expression by pathobionts (red) or bona fide pathogens[27].

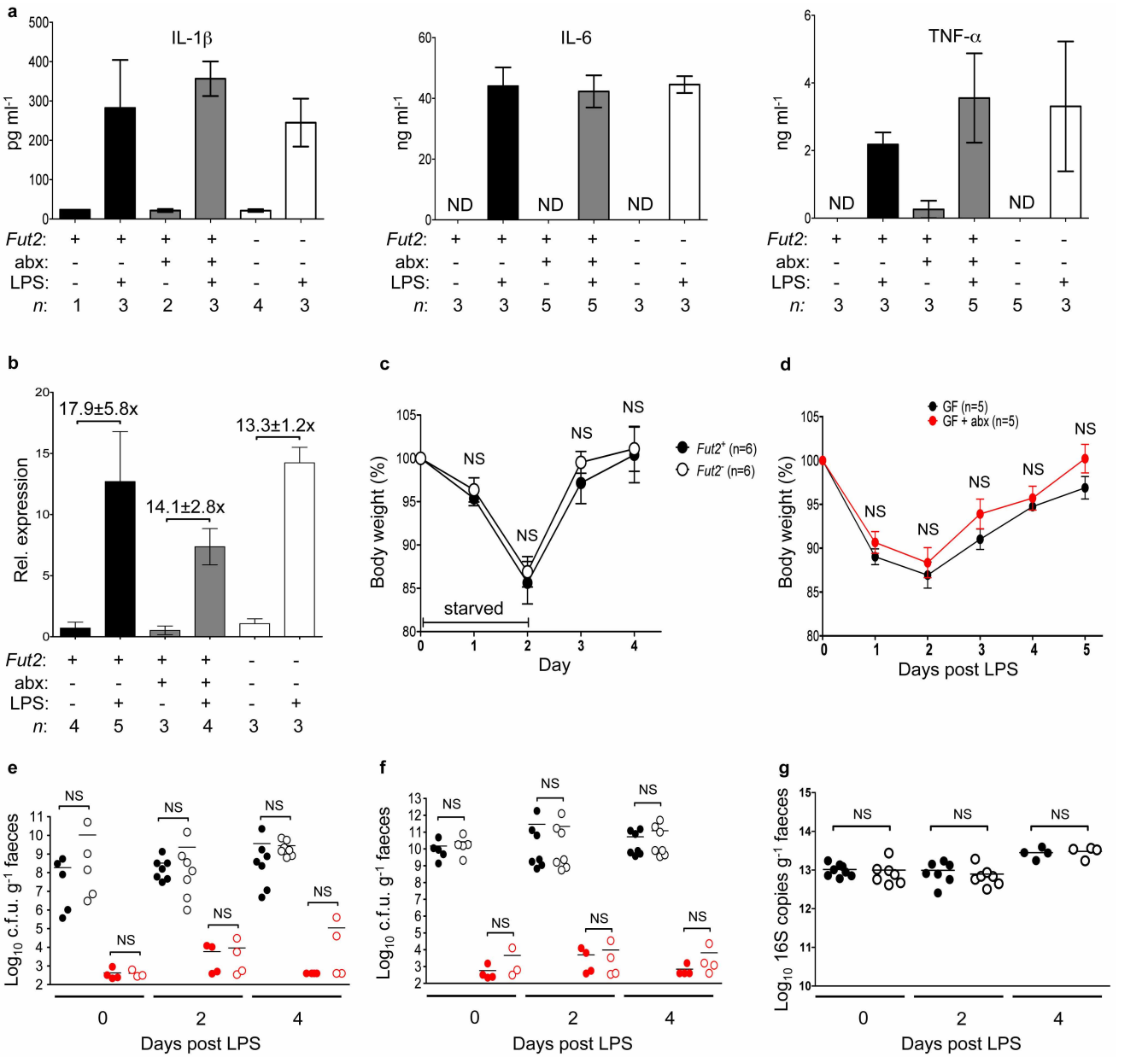

Extended Data Figure 4 | Consequences of LPS injection in Fut2-sufficient and Fut2-deficient BALB/c mice. **a**, Inflammatory cytokines IL-1β, IL-6 and TNF-α were measured by ELISA in sera of mice before or 2 h after injection with LPS (4 h for IL-1β). abx, mice on antibiotic water for 2 days before injection. Bars are mean ± s.e.m.; ND, not detected. Data are combined from three experiments. **b**, Expression of RegIIIγ (also regulated by the MyD88–IL23–IL22 pathway). Measurement by qPCR of *reg3g* gene expression in mid-small-intestine tissue, relative to *gapdh* (ddCt method). Numbers indicate mean fold change ± s.e.m. in LPS-treated versus untreated mice. Differences between LPS-treated Fut2^{+} and abx or Fut2^{-} levels are not significant ($P > 0.05$, two-tailed Student's *t*-test). Data are combined from three experiments. **c**, Weight loss and recovery is not different in Fut2$^{+/-}$ and Fut2$^{-/-}$ mice after simple starvation (mean ± s.e.m., $P > 0.05$ at all time points, two-tailed Student's *t*-test; NS, not significant). **d**, Lack of direct toxic effect of antibiotics (abx) measured as the weight loss of BALB/c GF animals treated with LPS i.p (mean ± s.e.m., $P > 0.05$ by two-tailed Student's *t*-test at all time points). Data are combined from two experiments. **e**–**g**, Similar total bacterial loads in Fut2$^{+/-}$ and Fut2$^{-/-}$ mice before and after LPS injection and antibiotic treatment. Total bacterial loads in faeces were estimated by plating on aerobic (**e**) and anaerobic (**f**) non-selective media, and by qPCR for 16S gene copies (**g**). There were no significant differences between Fut2-sufficient (filled circles) and Fut2-deficient (open circles) mice before or after LPS treatment (two-tailed Student's *t*-test). Circles indicate individual mice; horizontal lines indicate means; red circles indicate antibiotic-treated mice. Data are combined from three experiments.

a

Peptide source	Gene symbol	Function	Location	Abundance
Maltase glucoamylase	*mgam*	glycosidase	apical membrane	73
Sucrase-isomaltase	*si*	glycosidase	apical membrane	20
Glutamyl aminopeptidase	*enpep*	protease	apical membrane	10
Aminopeptidase N	*anpep*	protease	apical membrane	9
Fc of IgG binding protein	*fcgbp*	mucin and antibody binding	secreted	7
Isoform 1 of angiotensin-converting enzyme 2	*ace2*	protease	apical membrane	5
N-acetylated-alpha-linked acidic dipeptidase-like protein	*naaladl1*	protease	apical membrane	4
Mucin 13	*muc13*	protection/adhesion/ signaling?	apical membrane/ secreted	4
Isoform 1 of meprin A subunit beta	*mep1b*	protease	membrane	4
Chloride channel calcium activated 6	*clca6*	channel/channel regulator/protease?	apical membrane	3
Neutral ceramidase	*asah2*	lipidase	apical membrane	3
Isoform 2 of Mucin and cadherin-like protein	*mupcdh*	adhesion?	membrane	2
Integrin beta 1	*itgb1*	adhesion	membrane	2
Dipeptidyl peptidase 4	*dpp4*	protease	apical membrane	2

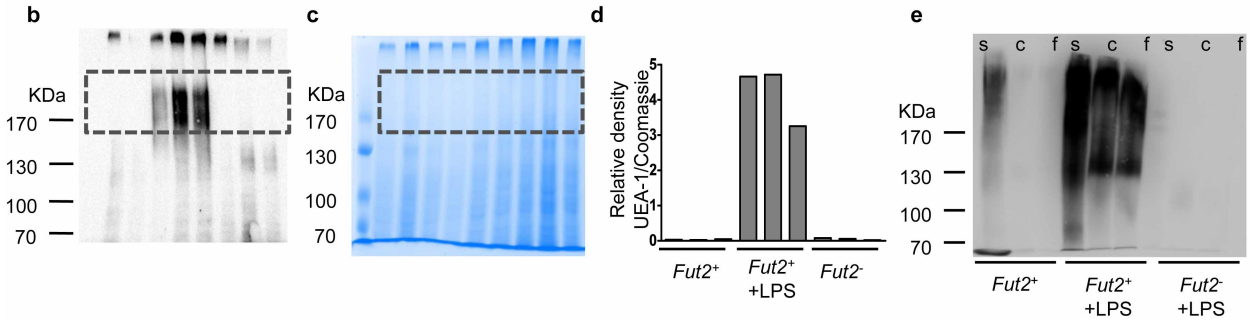

Extended Data Figure 5 | Fucosylated protein in IECs and gut contents. **a**, Proteins α(1,2)fucosylated in IECs after LPS injection identified by UEA-1 precipitation and mass spectrometry. Abundance is the number of peptide fragments attributed to each gene. **b**, IECs from Fut2^{+} untreated, Fut2^{+} LPS-treated, or Fut2^{-} untreated mice were isolated, and lysates separated by SDS–PAGE. α(1,2)fucosylated proteins were detected by blotting with UEA-1 lectin conjugated to horseradish peroxidase (HRP). **c**, Identical gel stained with Coomassie blue for total protein content. **d**, Relative density of the boxed area of each lane from **b** divided by the relative density in **c. e**, UEA-1 staining of luminal proteins as in Fig. 3c. Blot is overexposed to show absence of luminal fucosylated proteins in the LPS-treated, Fut2^{-} mouse. **b**–**e**, Data are representative of two independent experiments.

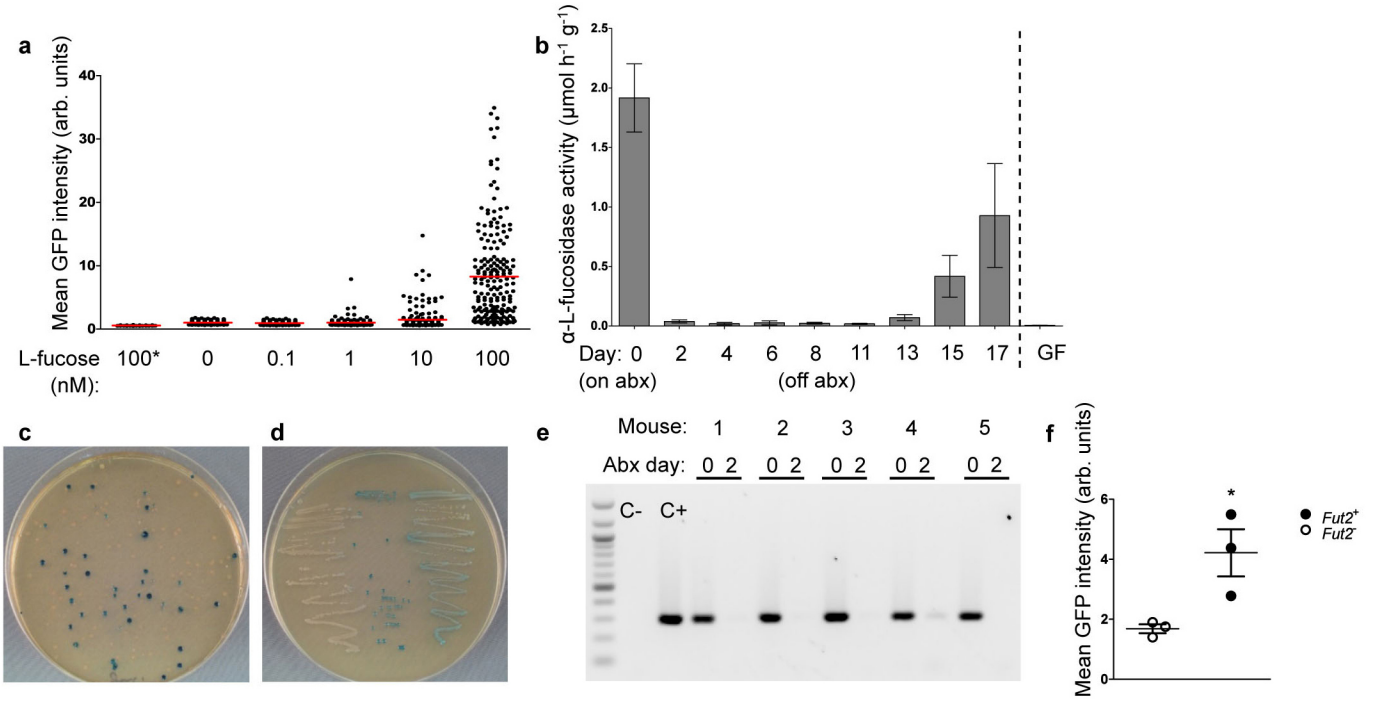

Extended Data Figure 6 | Generation of fucose-sensing reporter bacterial strains. **a**, Reporter *E. coli* were grown to stationary phase in minimal medium containing 10 mM glucose and the indicated concentrations of L-fucose (asterisk indicates promoter-less vector), and GFP fluorescence was measured. **b**, Fucosidase activity is dramatically reduced after 2 days of antibiotics (abx) treatment but recovers after cessation of treatment. Measurement of total α-L-fucosidase activity in faeces. Faecal supernatant was assayed for cleavage of 4-methylumbelliferyl-fucopyranoside substrate by fluorescence. $n = 5$ SPF antibiotics-treated, 3 GF mice. **c**, Faecal homogenates were plated anaerobically on BHIS agar containing 5-bromo-4-chloro-3-indolyl α-L-fucopyranoside, which forms a blue precipitate upon cleavage of the fucosyl residue. Both blue and white colonies are present. **d**, Pure cultures of *Bacteroides* species were streaked on the same medium as in **c**. *B. uniformis* (left) is not predicted to carry an α-L-fucosidase gene, and remains white; *B. acidifaciens* (middle) and *B. thetaiotaomicron* (right) both express fucosidase activity and develop blue colonies. **e**, Loss of *B. acidifaciens* from the faeces of mice treated with antibiotics (Abx) in water (PCR for the *gyrB* gene). C−, water control; C+, *B. acidifaciens* genomic DNA. **f**, Summary of reporter *E. coli* experiments in SPF mice (representative experiment is shown in Fig. 3e). Points are mean GFP fluorescence from all reporter bacteria measured in each of three independent experiments ($n = 65$ bacteria per mouse; $^*P < 0.05$, Student's t test).

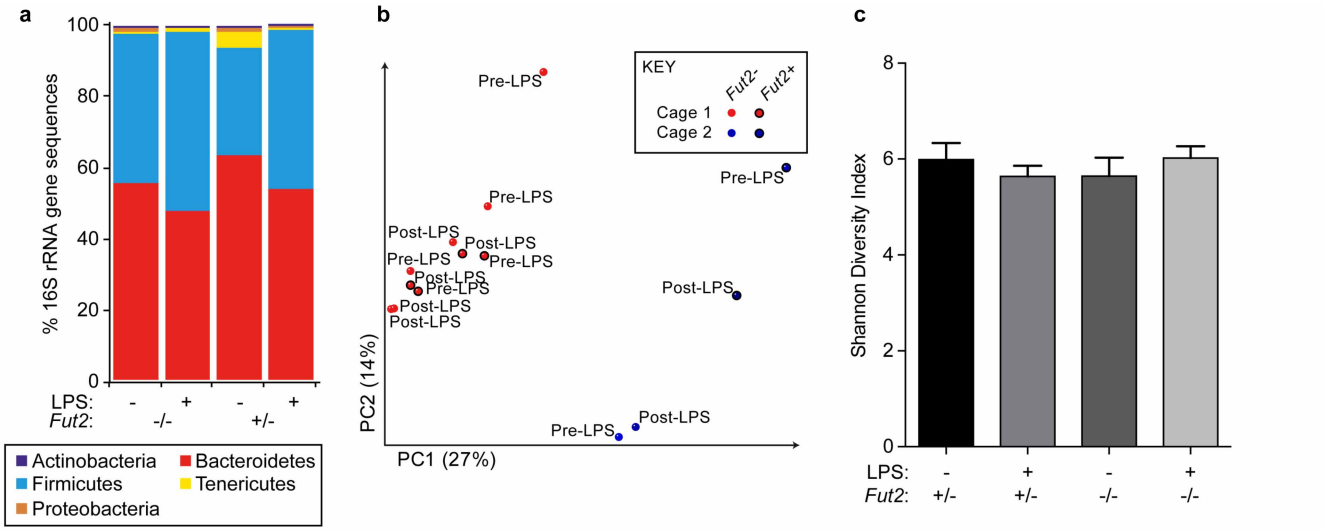

d

***Fut2*-positive**

KEGG module/pathway
ko00195 Photosynthesis
ko00531 Glycosaminoglycan degradation
ko03010 Ribosome
ko04142 Lysosome
M00045 Histidine degradation
M00095 C5 isoprenoid biosynthesis
M00149 Complex II succinate dehydrogenase
M00157 F type ATPase
M00164 ATP synthase
M00178 Ribosome bacteria
M00287 PTS system galactosamine specific II component
M00359 Aminoacyl tRNAbiosynthesis eukaryotes
M00360 Aminoacyl tRNAbiosynthesis prokaryotes

***Fut2*-negative**

KEGG module/pathway
ko00280 Valine leucine and isoleucine degradation
ko00310 Lysine degradation
ko00362 Benzoate degradation
ko02030 Bacterial chemotaxis
ko02040 Flagellar assembly
ko04626 Plant pathogen interaction
ko05110 Vibrio cholerae infection
M00018 Threonine biosynthesis
M00119 Pantothenate biosynthesis
M00200 Sorbitol mannitol transport system
M00302 2 Aminoethylphosphonate transport system

Extended Data Figure 7 | Microbial community structure is impacted by cohousing yet robust to host fucosylation and LPS exposure, whereas microbial gene expression depends on Fut2. **a**, Stable relative abundance of bacterial phyla across treatment groups and genotypes, as indicated by 16S rRNA gene sequencing. Values represent the mean abundance of phyla found at >1% relative abundance in at least one sample. **b**, Unweighted UniFrac analysis of the gut microbiota of Fut2-deficient (no outline) and Fut2-sufficient (black outline) mice. Points are coloured based on kinship and labelled by time point (before or after LPS exposure). Results are based on 180,000 randomly selected 16S rRNA gene sequences per sample. **c**, Microbial diversity as measured by the Shannon diversity index (n = 178,100 sequences per sample). Values are mean ± s.e.m. (n = 3 $Fut2^{+}$, 4 $Fut2^{-}$ mice per time point). **d**, KEGG modules and pathways expressed in microbiota at higher levels after LPS exposure in Fut2-positive (left) and Fut2-negative mice (right) (n = 3 per group; Humann/LefSe analysis; LDA >2).

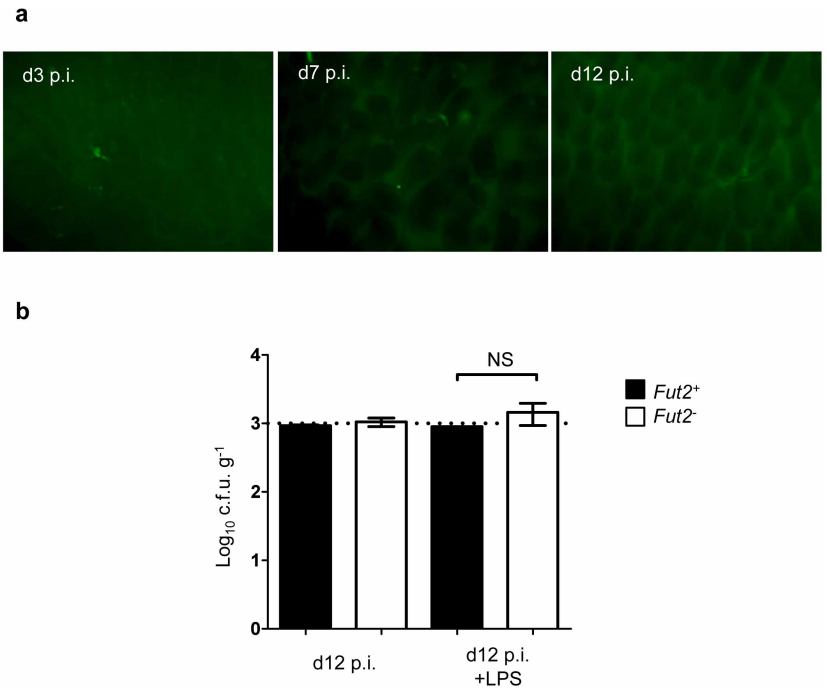

Extended Data Figure 8 | Lack of indicible fucosylation and small intestine colonization in *C. rodentium*-infected mice. **a**, *C. rodentium* causes no small intestine fucosylation in SPF mice at day (d)3, day 7, or day 12 post-infection (p.i.). **b**, Small intestine colonization by *C. rodentium* is low regardless of Fut2 expression and LPS treatment. Small intestine contents were removed by gentle squeezing, homogenized in PBS, and plated. Data are shown as mean ± s.e.m.; $n = 4$. NS, not significant. Dotted line shows the limit of detection. Data are representative of two experiments.

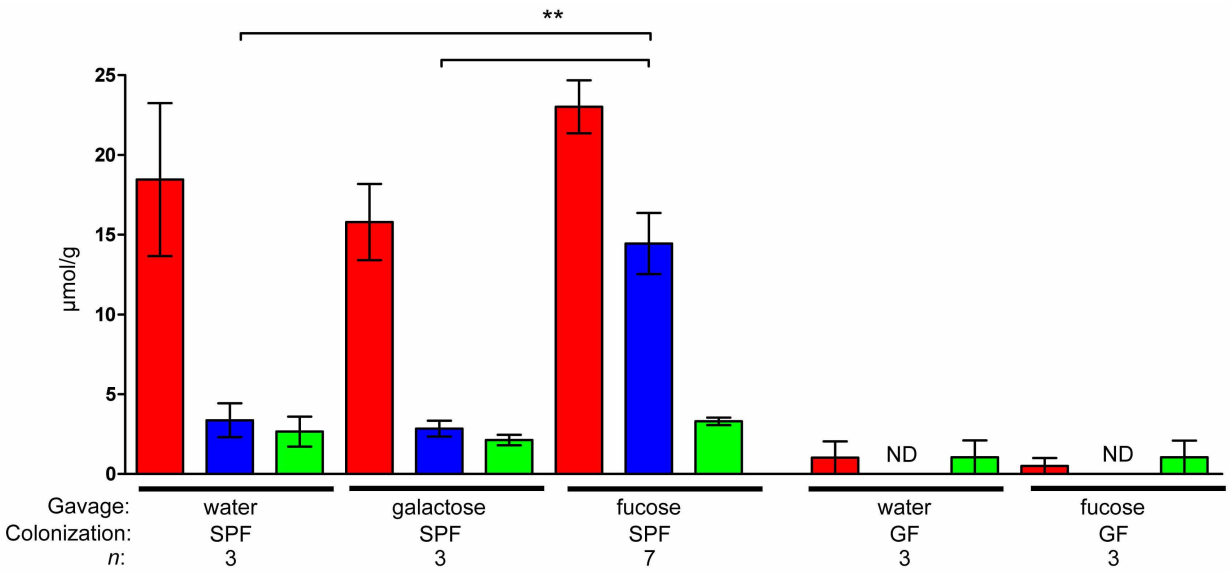

Extended Data Figure 9 | Effect of exogenous fucose on caecal short-chain fatty acid levels. Caecal short-chain fatty acids were measured after gavaging starved mice with the indicated sugars (100 mM concentration). Fucose gavage leads to increased propionate production in SPF but not GF mice. Data are shown as mean ± s.e.m. $^{**}P < 0.01$, Student's two-tailed *t*-test. ND, not detected. Data are combined from three experiments.